Adipose Tissue Dendritic Cells Are Independent Contributors to Obesity-Induced Inflammation and Insulin Resistance

Kae Won Cho,*,†,[1] Brian F. Zamarron,*,‡,[1] Lindsey A. Muir,* Kanakadurga Singer,*,‡ Cara E. Porsche,*,‡ Jennifer B. DelProposto,* Lynn Geletka,* Kevin A. Meyer,[§] Robert W. O'Rourke,[§,¶] and Carey N. Lumeng*,‡,‖

Dynamic changes of adipose tissue leukocytes, including adipose tissue macrophage (ATM) and adipose tissue dendritic cells (ATDCs), contribute to obesity-induced inflammation and metabolic disease. However, clear discrimination between ATDC and ATM in adipose tissue has limited progress in the field of immunometabolism. In this study, we use CD64 to distinguish ATM and ATDC, and investigated the temporal and functional changes in these myeloid populations during obesity. Flow cytometry and immunostaining demonstrated that the definition of ATM as F4/80$^+$CD11b$^+$ cells overlaps with other leukocytes and that CD45$^+$CD64$^+$ is specific for ATM. The expression of core dendritic cell genes was enriched in CD11c$^+$CD64$^-$ cells (ATDC), whereas core macrophage genes were enriched in CD45$^+$CD64$^+$ cells (ATM). CD11c$^+$CD64$^-$ ATDCs expressed MHC class II and costimulatory receptors, and had similar capacity to stimulate CD4$^+$ T cell proliferation as ATMs. ATDCs were predominantly CD11b$^+$ conventional dendritic cells and made up the bulk of CD11c$^+$ cells in adipose tissue with moderate high-fat diet exposure. Mixed chimeric experiments with *Ccr2*$^{-/-}$ mice demonstrated that high-fat diet–induced ATM accumulation from monocytes was dependent on CCR2, whereas ATDC accumulation was less CCR2 dependent. ATDC accumulation during obesity was attenuated in *Ccr7*$^{-/-}$ mice and was associated with decreased adipose tissue inflammation and insulin resistance. CD45$^+$CD64$^+$ ATM and CD45$^+$CD64$^-$CD11c$^+$ ATDCs were identified in human obese adipose tissue and ATDCs were increased in s.c. adipose tissue compared with omental adipose tissue. These results support a revised strategy for unambiguous delineation of ATM and ATDC, and suggest that ATDCs are independent contributors to adipose tissue inflammation during obesity. ***The Journal of Immunology*****, 2016, 197: 3650–3661.**

Obesity-induced inflammation is a potent contributing factor to the development of type 2 diabetes and metabolic dysfunction associated with insulin resistance. Metabolic inflammation (metainflammation) is driven largely by the induction of inflammation in obese adipose tissue and is regulated by a network of adipose tissue leukocytes (1, 2). The inflammatory components in adipose tissue include both innate and adaptive immune cells that are resident in adipose tissue in the lean state and undergo both qualitative and quantitative changes with obesity. Myeloid cells were among the first leukocytes identified as being deranged in obese adipose tissue and in the circulation (3). Obese children as young as 3 y of age have increased circulating neutrophils indicating an early influence of obesity on myeloid cell regulation (4). Associations among classical monocytes (Ly6c^{hi} in mice and CD14$^+$CD16$^+$ in humans), adipose tissue macrophage (ATM) content, and insulin resistance suggest a mechanistic contribution of myeloid cells to the development of metabolic disease (5, 6). Furthermore, obesity-induced activation of neutrophils and macrophages in adipose tissue is required for insulin resistance in obese mice and correlates with metabolic disease in humans (7, 8).

ATMs are a dominant innate immune cell in adipose tissue and can comprise up to 40% of the nonadipocyte stromal vascular fraction (SVF) in obese adipose tissue (9–11). Murine ATMs have been primarily defined as F4/80$^+$CD11b$^+$, and with obesity F4/80$^+$CD11b$^+$CD11c$^+$ ATMs accumulate (9, 12). The importance

*Department of Pediatrics and Communicable Diseases, University of Michigan Medical School, Ann Arbor, MI 48109; †Soonchunhyang Institute of Medi-bio Science, Soonchunhyang University, Cheonan-si, Chungcheongnam-do, 31151, Korea; ‡Graduate Program in Immunology, University of Michigan Medical School, Ann Arbor, MI 48109; §Department of Surgery, University of Michigan Medical School, Ann Arbor, MI 48109; ¶Department of Surgery, Ann Arbor Veteran's Administration Hospital, Ann Arbor, MI 48109; and ‖Molecular and Integrative Physiology, University of Michigan Medical School, Ann Arbor, MI 48109

[1]K.W.C. and B.F.Z. contributed equally to this work.

ORCIDs: 0000-0001-7512-6722 (K.W.C.); 0000-0001-6549-4230 (B.F.Z.); 0000-0002-1756-0325 (L.A.M.); 0000-0001-8278-3800 (K.S.); 0000-0003-1581-5571 (C.E.P.); 0000-0002-4038-4198 (R.W.O.); 0000-0003-0303-6204 (C.N.L.).

Received for publication May 9, 2016. Accepted for publication August 31, 2016.

This work was supported by National Institutes of Health Grant DK090262 (to C.N.L.), American Diabetes Association Grant 07-12-CD-08 (to C.N.L.), National Research Foundation of Korea Grant NRF-2014R1A1AA1038426 (to K.W.C.), Korean Diabetes Association Grant 2015F-3 (to K.W.C.), National Institutes of Health National Institute of Allergy and Infectious Diseases Experimental Training in Immunology Grant T32 AI007413-19 (to B.F.Z.), National Institute of Diabetes and Digestive and Kidney Diseases Grant F31 DK103524 (to B.F.Z.), an American Heart Association Predoctoral Fellowship (to B.F.Z.), National Institute of Diabetes and Digestive and Kidney Diseases Grants T32 DK101357 and F32 DK105676 (to L.A.M.), and National Institutes of Health Grants 14SDG17890004 and K08DK101755 (to K.S.).

The data presented in this article have been submitted to the National Center for Biotechnology Information's Gene Expression Omnibus (https://www.ncbi.nlm.nih.gov/geo/query/acc.cgi?acc=GSE85846) under accession number GSE85846.

Address correspondence and reprint requests to Dr. Carey N. Lumeng, University of Michigan Medical School, 109 Zina Pitcher Place, 2057 Biomedical Sciences Research Building, Ann Arbor, MI 48109-2200. E-mail address: clumeng@umich.edu

The online version of this article contains supplemental material.

Abbreviations used in this article: ATDC, adipose tissue dendritic cell; ATM, adipose tissue macrophage; cATDC, conventional ATDC; cDC, conventional DC; CLS, crownlike structure; DC, dendritic cell; eWAT, epididymal adipose tissue; HFD, high-fat diet; HOMA-IR, homeostasis model assessment–estimated insulin resistance; iWAT, inguinal adipose tissue; MHCII, MHC class II; ND, normal diet; OM, omental/visceral adipose tissue; SVF, stromal vascular fraction; WT, wild type.

of CD11c$^+$ ATMs has been emphasized in numerous studies in mice and humans (6, 12, 13). Obesity induces CD11c expression in macrophages and circulating monocytes to enhance their trafficking into adipose tissue (14). Ablation of CD11c$^+$ cells attenuates adipose tissue inflammation and improves glucose tolerance without changes in body weight (15, 16). CD11c$^+$ ATMs have been described as having a metabolically active phenotype with lysosomal activation and characteristics of classically activated M1 macrophages (10, 11). In addition to classical innate immune cytokine production, ATMs express high levels of MHC class II (MHCII) and are active APCs that shape the expansion of conventional Th1 CD4$^+$ T cells, induction of effector/memory T cells, and the attenuation of regulatory T cells (16–18).

The induction of CD11c$^+$ cells in adipose tissue suggests the possibility that adipose tissue dendritic cells (ATDCs) may play a role in obesity-associated inflammation. Adipose tissue CD1c expression correlates with homeostasis model assessment–estimated insulin resistance (HOMA-IR) in clinical studies, suggesting an association between ATDC expansion and insulin resistance (19). However, because CD11b and F4/80 expression overlaps between macrophages and dendritic cells (DCs), it has been difficulty to clarify the contribution of ATDC to adipose tissue inflammation. In mouse obesity models, ATDCs have been defined as CD11b$^+$CD11c$^+$, CD11c$^+$F4/80^{lo}, CD11c$^+$, or CD11c$^+$ F4/80$^{neg\text{-}lo}$ cells depending on the study (19–24). Based on these definitions, conventional DCs (cDCs) and plasmacytoid (B220$^+$) dendritic cells in adiopose tissue have been reported, but how these overlap with the previously defined CD11c$^+$ and CD11c$^-$ ATMs has not been clarified. Ex vivo, ATDC can induce a Th17 profile in T cells that may explain the associations between Th17 cytokines and insulin resistance (19). Perforin$^+$ ATDCs can contribute to the regulation of adipose tissue expansion by controlling adipose tissue T cell clonal expansion (23). GM-CSF–dependent DCs contribute to adipose tissue expansion in lean animals (24). CD64$^-$ ATDCs in perinodal adipose tissue play a role in Ag capture and presentation to lymph nodes, but how this interfaces with metabolic inflammation in obesity is unclear (22).

Almost all studies of murine ATM have used F4/80 as the primary marker despite its known expression on nonmacrophage leukocytes such as DCs and eosinophils. The Immunologic Genome Consortium identified markers including CD64 and MerTK that improve the specificity of tissue macrophage phenotyping in several tissues including adipose tissue (25). The use of CD64 has been beneficial in untangling macrophage and DC identity and diversity in the gut (26, 27). Therefore, we used CD64 to revisit the F4/80 ATM phenotyping strategy in hopes of improving our understanding of the dynamics and functions of ATM and ATDC in obesity. We support the use of CD64 as a highly specific ATM marker and that CD64$^-$CD11c$^+$ staining defines a pure population of bona fide myeloid ATDCs present in lean and obese states in mice and humans. We distinguish CD11c$^+$ ATMs and CD11c$^+$ ATDCs induced by obesity with distinct gene expression profiles and lipid storage capacity. Using competitive reconstitution experiments, we found CD11c$^+$ ATM accumulation to be CCR2 dependent, whereas ATDCs were only partially CCR2 dependent. With moderate high-fat diet (HFD) feeding, ATDCs are the dominant CD11c$^+$ cell population induced in adipose tissue, and *Ccr7*$^{-/-}$ mice with decreased ATDC content were protected from insulin resistance. This work increases the resolution by which adipose tissue myeloid cells can be identified and suggests that ATDCs are an independent contributor to obesity-induced adipose tissue inflammation.

Materials and Methods

Animal studies

CD45.1 and CD45.2 C57BL/6J, CCR 7$^{-/-}$ [B6.129P2(C)-CCR7tm1Rfor/J], and OT-II [B6.Cg-Tg(TcraTcrb)425Cbn/J] mice were obtained from Jackson Laboratories. *Ccr2*$^{-/-}$ and *Csf2*$^{-/-}$ mice were kindly provided by Dr. Beth Moore and Dr. John Osterholzer at the University of Michigan, respectively. Male mice were fed a normal diet (ND; 4.5% fat; LabDiet) ad libitum or fed an HFD (60% fat; Research Diets) ad libitum beginning at 6 wk of age. All animal experiments were approved by the University Committee on Use and Care of Animals at the University of Michigan and conducted in compliance with the Institute of Laboratory Animal Research Guide for the Care and Use of Laboratory Animals.

Bone marrow transplantation

Competitive bone marrow transplants were performed as described previously (28). In brief, bone marrow cells were isolated from donor groups (CD45.1$^+$ CCR2$^{+/+}$ and CD45.2$^+$ CCR2$^{-/-}$) and mixed in a 1:1 ratio. Six-week-old CD45.1 mice were lethally irradiated (900 rad) and i.v. injected 6 h after irradiation with 10×10^6 cells of the mixed bone marrow donor cells resuspended in 150 μl of PBS. Bone marrow reconstitution efficiency was evaluated by examining peripheral blood leukocyte CD45.1$^+$/CD45.2$^+$ ratios at 6 wk after transplantation, and recipient animals were fed either an ND or HFD for 15 wk.

Human adipose tissue

Human omental and s.c. adipose tissues were collected intraoperatively from patients undergoing bariatric surgery at the University of Michigan and the Ann Arbor VA Hospital. All human use protocols were approved by the University of Michigan and Ann Arbor VA Hospital Institutional Review Boards.

Immunofluorescence microscopy

Immunofluorescence staining was performed as described previously (29) using the following Abs: anti-CD64 (X54-5/7.1), anti-F480 (A3-1), anti-Mgl1 (MP23), anti-CD11c (N418), anti-Mac2 (M3/38), and anti-Caveolin (2297). Images were collected using an Olympus Fluoview 100 laser scanning confocal microscope.

SVF isolation and flow cytometry analysis

SVF cells were isolated as described previously (30). Cells were incubated in Fc block for 10 min on ice and stained with indicated Abs for 30 min at 4°C. Abs for flow cytometry are provided in Supplemental Table I. Live/dead fixable violet staining kits (Life Technology) and BODIPY (Life Technology) were used according to the manufacturers' instruction. Cells were analyzed on a FACSCanto II Flow Cytometer (BD Biosciences) using FlowJo 10.6 software (Tree Star). For FACS, SVFs were suspended in RPMI 1640/2% FBS and purified by FACSAria III (BD Biosciences). Fluorescence minus one controls were used to confirm Siglec-F, Ly6G, and CD11c expression in SVF analyses in mice and humans in at least three independent experiments.

Microarray and real-time RT-PCR

Male C57BL/6 mice fed ND or HFD for 20 wk were used for gene expression analysis in macrophages and DCs. Cells were identified as M1 macrophages (CD45$^+$CD11c$^+$CD64$^+$), M2 macrophages (CD45$^+$CD11c$^-$CD64$^+$), or DCs (CD45$^+$CD11c$^+$CD64$^-$) and sorted using a BD FACSAria III cell sorter. Microarray analyses were carried out as previously described (31). RNA was extracted using QIAzol (Qiagen) and amplified and hybridized on the Affymetrix Mouse Gene 2.1 ST array. RNA quality was assessed on Agilent Bioanalyzer Picochip. After quality-control assessments, probe sets with unadjusted $p \leq 0.05$ were identified. Differences in gene expression were identified and analysis was performed through the University of Michigan Microarray Core using affy, limman, and affy PLM packages of bioconductor implemented in the R statistical environment. The data discussed in this publication have been deposited in National Center for Biotechnology Information's Gene Expression Omnibus and are accessible through Gene Expression Omnibus Series accession number GSE85846 (https://www.ncbi.nlm.nih.gov/geo/query/acc.cgi?acc=GSE85846).

For real-time PCR, RNA from tissues and cells was prepared using RNeasy Midi Kits (QIAGEN), and cDNA was generated using high-capacity cDNA reverse transcription kits (Applied Biosystems). Real-time RT-PCR analyses were done in duplicate on the ABI PRISM 7900 Sequence Detector TaqMan System with the SYBR Green PCR kit as instructed by the manufacturer (Applied Biosystems). Primers are shown in

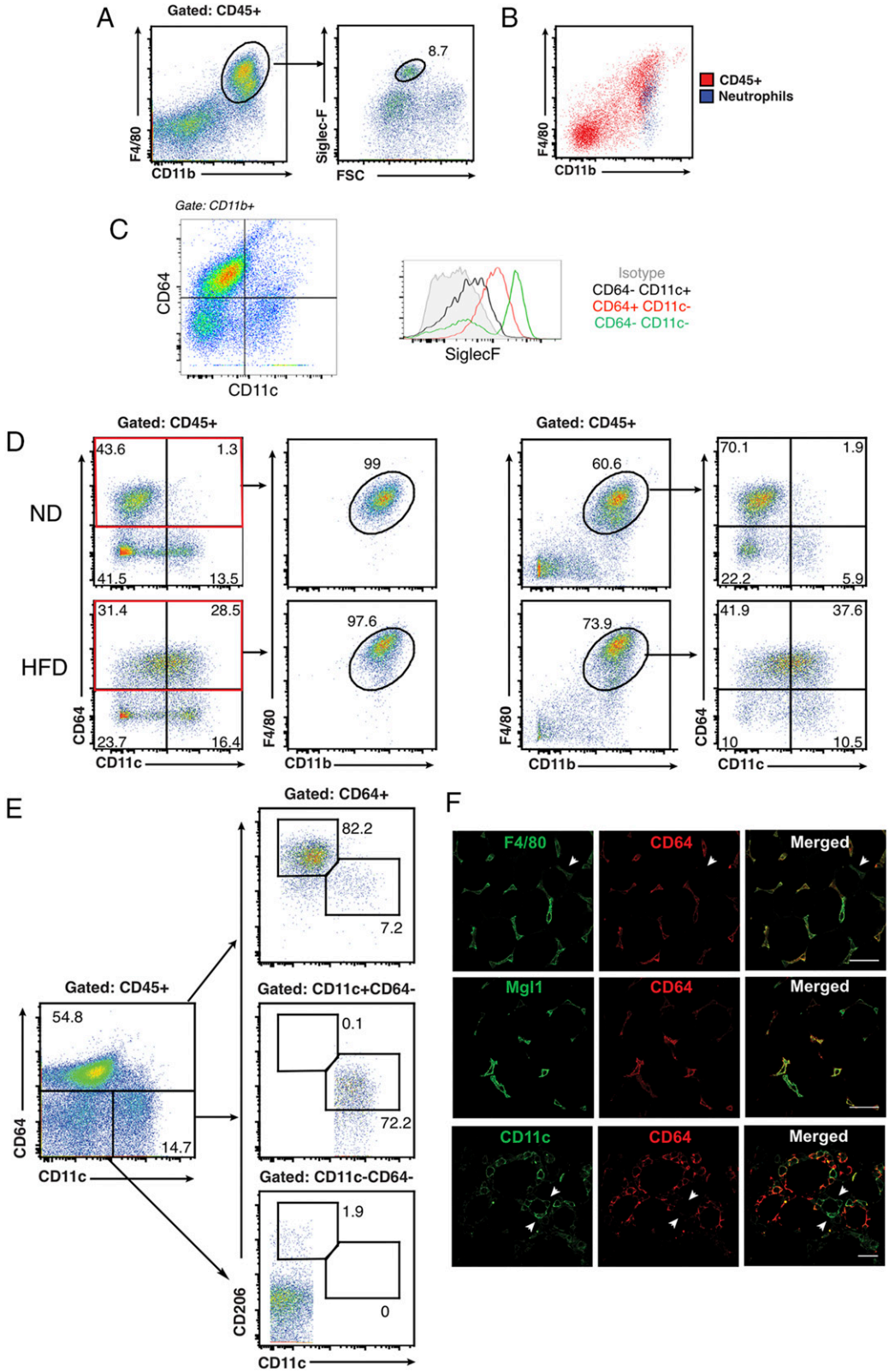

FIGURE 1. CD64 is a specific ATM marker in lean and obese mice. Analysis of SVF from eWAT in C57BL/6 mice were fed with ND or HFD for 20 wk. (**A**) Flow cytometry analysis of eosinophils (siglec-F$^+$ and high side scatter) on CD11b$^+$F480$^+$ cells after gating CD45$^+$ SVFs from lean mice. (**B**) Overlap between F480$^+$ CD45$^+$ SVF cells (red) and neutrophils (blue) from obese mice. (**C**) Analysis of Siglec-F expression in CD64 stratified SVF cells. (**D**) Comparison of CD64 and F4/80 staining in SVF from ND- and HFD-fed mice. (**E**) Flow analysis of CD11c and CD206 expression in CD64$^+$ (top), CD11c$^+$CD64$^-$ (middle), and CD11c$^-$CD64$^-$ (bottom) SVF cells from lean mice. (**F**) Immunofluorescence analysis of CD64$^+$ (red) cells in eWAT from HFD-fed mice. Scale bar, 100 μm. Arrowheads indicate CD64$^-$ SVF cells. Data are representative of at least three independent experiments with three mice per group.

Supplemental Table II. *Arbp* or 18S was used as a housekeeping gene/internal standard for normalization. Relative expression was determined using the standard $2^{-\Delta\Delta Ct}$ method.

CFSE dilution assay

Ag-specific T cell activation assay was performed as previously described (18). In brief, FACS-sorted cells were grown in 90-well U-bottom plates and then pulsed with 100 μg/ml whole OVA (Thermo Scientific). $CD4^+$ T cells were isolated from the spleen of OT-II mice using $CD4^+$ T cell negative selection kits (Miltenyi Biotec). $CD4^+$ T cells were labeled with 2 μmol/l CFSE and added to Ag-pulsed cells at a 1:1 ratio. After 5 d, T cells were stained for flow cytometry, and CFSE dilution was examined in viable $CD3^+CD4^+$ lymphocytes.

Metabolic evaluation

Body weights were measured weekly. Blood glucose and plasma insulin were measured by glucometer and ELISA kit (Crystal Chem), respectively.

Statistical analysis

Data are expressed as means ± SEM. Statistical differences were assessed using a two-tailed *t* test or ANOVA (with Tukey's posttest analysis), using GraphPad Prism software. A p value <0.05 was considered statistically significant.

Results

CD64 distinguishes ATMs from eosinophils, neutrophils, and ATDCs in lean and obese mice

Our group and others have defined ATM as $CD45^+F4/80^+CD11b^+$ cells in the SVF despite the potential for nonmacrophage $F4/80^+$ cell contamination. Costaining with markers for eosinophils (Siglec-F) and neutrophils (Ly6G) demonstrated that these cells are present within the $CD45^+F4/80^+CD11b^+$ fraction in both lean and obese mice (Fig. 1A, 1B). We examined the utility of CD64 as a more specific marker of ATM in lean and obese (HFD fed for 10–12 wk) mice. Adipose tissue eosinophils were $CD64^-$ in both lean and obese mice (Fig. 1C), with $CD64^+$ macrophages showing intermediate Siglec-F expression. Using CD64 and CD11c, lean mice demonstrated prominent populations of $CD64^+CD11c^-$ (putative ATM) and $CD64^-CD11c^+$ cells (putative ATDC) with rare $CD64^+CD11c^+$ cells (Fig. 1D). In obese mice, there was an increase in $CD64^+CD11c^+$ ($CD11c^+$ ATM), whereas distinct $CD64^+CD11c^-$ and $CD64^-CD11c^+$ cells were still identifiable. All $CD45^+CD64^+$ cells expressed CD11b and F4/80, indicating that CD64 is capable of labeling cells that have been previously

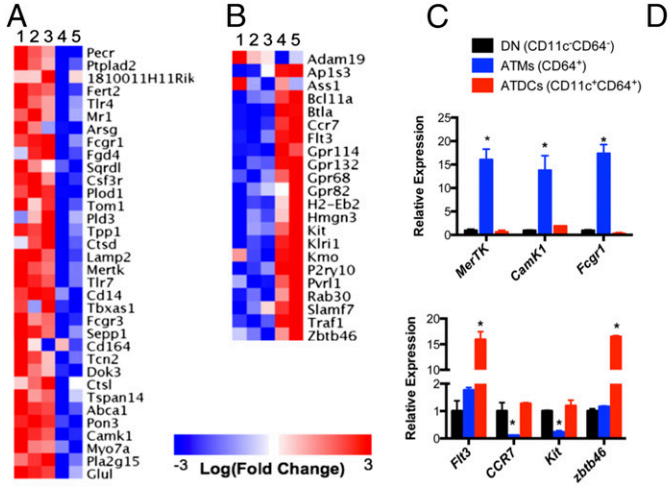

D

Gene Sets Enriched in ATDC	NES	NOM p-val	FDR q-val
KEGG_GRAFT_VERSUS_HOST_DISEASE	-2.26066	0.00000	0
REACTOME_IMMUNOREGULATORY_INTERACTIONS_BETWEEN_A_LYMPHOID_AND_A_NON_LYMPHOID_CELL	-2.25391	0.00000	0
BIOCARTA_NO2IL12_PATHWAY	-2.12644	0.00000	6.97E-04
KEGG_TYPE_I_DIABETES_MELLITUS	-2.05391	0.00000	0.002531
BIOCARTA_IL12_PATHWAY	-2.05373	0.00000	0.002391
REACTOME_OLFACTORY_SIGNALING_PATHWAY	-2.04716	0.00000	0.002361
BIOCARTA_TH1TH2_PATHWAY	-1.99419	0.00000	0.005374
BIOCARTA_CTLA4_PATHWAY	-1.98406	0.00000	0.0061
KEGG_ANTIGEN_PROCESSING_AND_PRESENTATION	-1.97844	0.00000	0.006526
KEGG_OLFACTORY_TRANSDUCTION	-1.96737	0.00000	0.007186
KEGG_ALLOGRAFT_REJECTION	-1.92319	0.00195	0.01207
REACTOME_GPCR_LIGAND_BINDING	-1.85978	0.00000	0.023854

Gene Sets Enriched in CD11c+ ATM	NES	NOM p-val	FDR q-val
KEGG_COMPLEMENT_AND_COAGULATION_CASCADES	1.988237	0.00000	0.053184
KEGG_N_GLYCAN_BIOSYNTHESIS	1.922015	0.00000	0.038621
KEGG_VALINE_LEUCINE_AND_ISOLEUCINE_DEGRADATION	1.886619	0.00000	0.04483
REACTOME_PRE_NOTCH_TRANSCRIPTION_AND_TRANSLATION	1.868543	0.00000	0.046561
REACTOME_TRANSPORT_OF_VITAMINS_NUCLEOSIDES_AND_RELATED_MOLECULES	1.837863	0.00225	0.058041
REACTOME_METABOLISM_OF_VITAMINS_AND_COFACTORS	1.821832	0.00000	0.062772
BIOCARTA_IGF1MTOR_PATHWAY	1.811142	0.00198	0.065287
KEGG_LYSOSOME	1.808807	0.00000	0.065976
BIOCARTA_COMP_PATHWAY	1.803181	0.00615	0.068747
REACTOME_BRANCHED_CHAIN_AMINO_ACID_CATABOLISM	1.799137	0.00000	0.070741
REACTOME_SIGNALING_BY_NOTCH1	1.788524	0.00225	0.072817
REACTOME_CIRCADIAN_CLOCK	1.785876	0.00230	0.072729

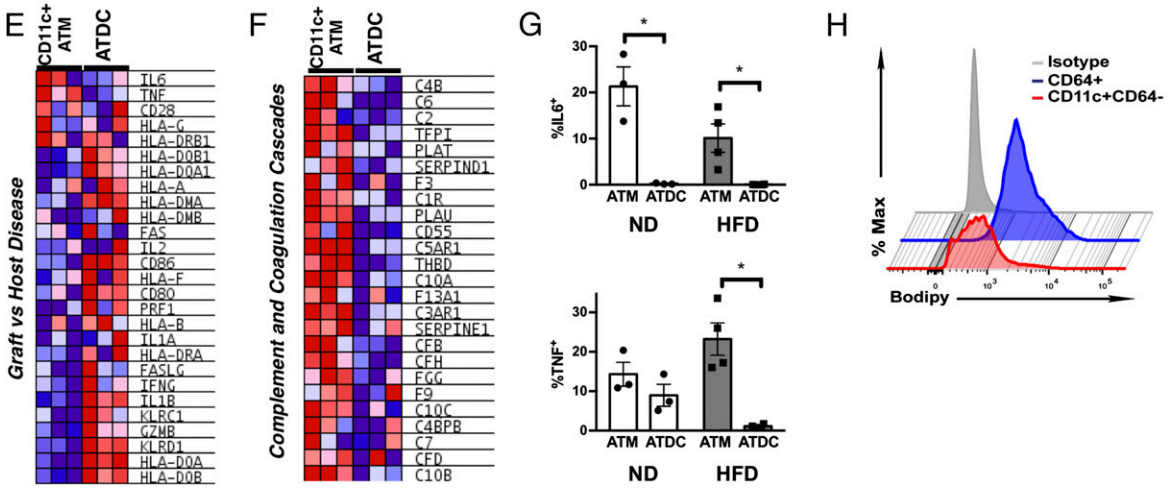

FIGURE 2. Gene expression profiling of ATMs and ATDCs. Microarray analysis heat map of ImmGen (**A**) macrophage core signature genes and (**B**) DC core signature genes from adipose tissue myeloid cells. Lane 1: lean ATM $CD11c^-CD64^+$; lane 2: obese ATM $CD11c^-CD64^+$; lane 3: obese ATM $CD11c^+CD64^+$; lane 4: lean ATDC $CD11c^+CD64^-$; and lane 5: obese ATDC $CD11c^+CD64^-$. (**C**) Quantitative PCR analysis of macrophage-specific genes (upper panel) and DC-specific genes (lower panel) in $CD11c^-CD64^-$ double negative (DN), $CD64^+$ (ATM), and $CD11c^+CD64^-$ (ATDC) cells from eWAT of obese mice. (**D**) Gene Set Enrichment Analysis pathways enriched in ATDCs and $CD11c^+$ ATMs. Heat maps shown for differentially expressed genes for (**E**) graft-versus-host disease and (**F**) complement and coagulation cascade. (**G**) Intracellular cytokine staining for ATMs and ATDCs from ND- and HFD-fed mice eWAT. (**H**) Flow cytometry analysis of intracellular lipid content in $CD64^+$ ATMs and $CD11c^+CD64^-$ ATDCs from obese mice. Data are from two independent experiments with three mice per group. $^*p < 0.05$.

identified as CD45$^+$F4/80$^+$CD11b$^+$ATM. However, >20% of CD45$^+$F4/80$^+$CD11b$^+$ cells in both lean and obese adipose tissue were CD64$^-$, further supporting the presence of nonmacrophage F4/80$^+$ cells.

F4/80$^+$CD11b$^+$ ATMs in lean mice have high expression of markers for alternatively activated macrophages such as CD206 and CD301/Mgl1 (32). In lean mice, of the CD64$^+$ population, 82% of them were CD206$^+$ with rare CD64$^-$CD11c$^-$CD206$^+$ cells identified (Fig. 1E). The ability of CD64 to identify ATM was further confirmed with immunofluorescence microscopy. There was colocalization of F4/80 and CD64 staining in lean mice; however, F4/80$^+$ cells were also identified that did not stain for CD64. Colocalization between Mgl1 and CD64 staining was prominent in lean adipose tissue (Fig. 1F). In obese mice, where CD11c$^+$ cells accumulate, colocalization between CD11c and CD64 was observed. However, distinct populations of CD11c$^+$ cells were identified that did not stain positive for CD64 in obese adipose tissue. Mac2 and CD64 staining showed significant overlap especially in crownlike structures (CLS) where dense myeloid cell accumulation is known to occur.

Gene expression profiling supports distinguishing ATMs and ATDCs based on CD64

These initial studies suggest that ATMs are more stringently defined as CD45$^+$CD64$^+$CD11c$^{+/-}$ cells and may permit the delineation of CD45$^+$CD64$^-$CD11c$^+$ ATDCs. To validate this, we performed microarray analysis on RNA from FACS-sorted CD45$^+$CD64$^+$CD11c$^-$, CD45$^+$CD64$^+$CD11c$^+$, and CD45$^+$CD64$^-$CD11c$^+$ cells from lean and obese mice. Because of their low numbers, CD64$^+$CD11c$^+$ in lean mice were not included in the analysis. When compared

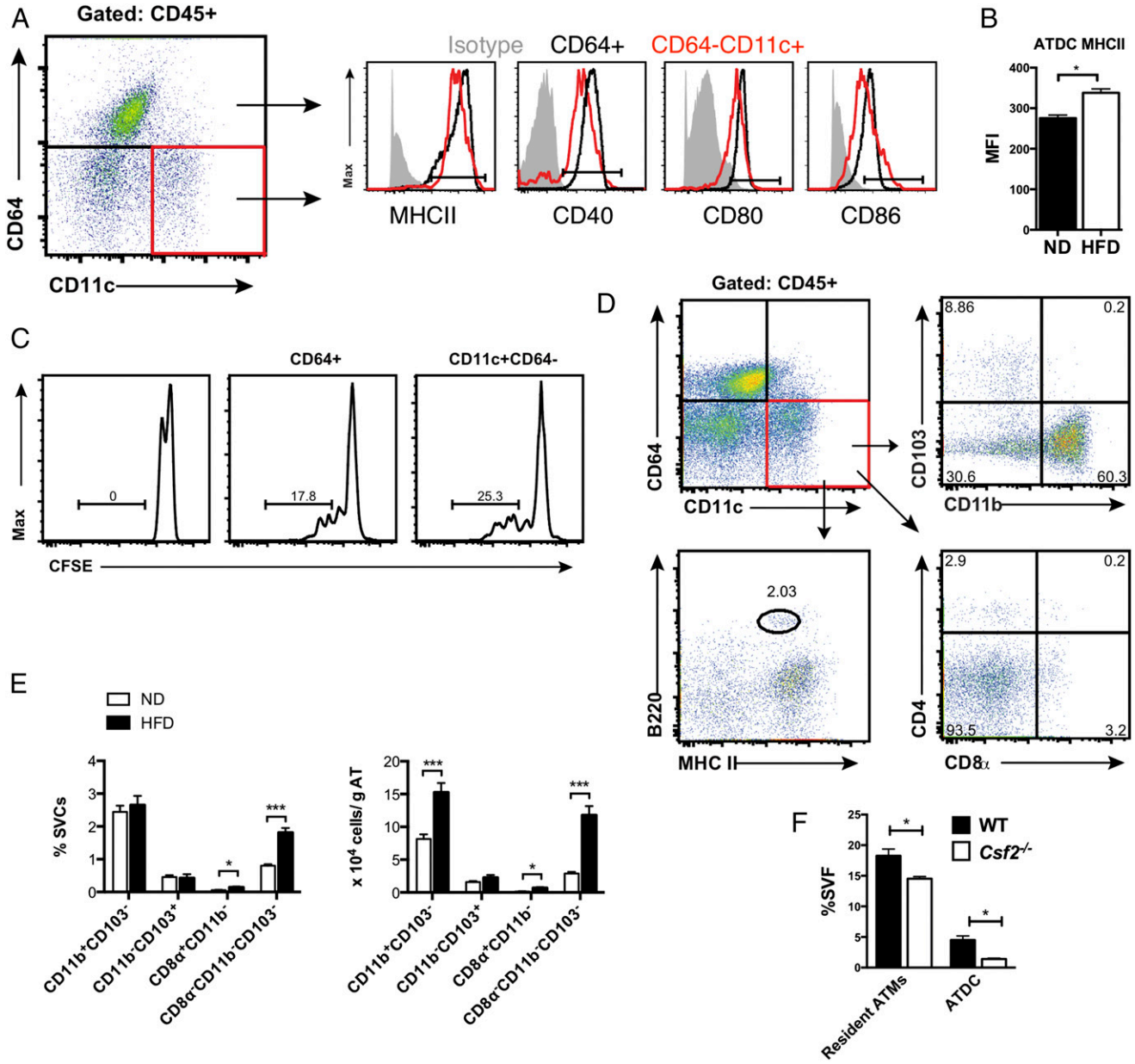

FIGURE 3. Myeloid DCs predominate in adipose tissue. (**A**) Flow cytometry analysis of MHCII and costimulatory molecules in CD64$^+$ ATMs (blue) and CD11c$^+$CD64$^-$ ATDCs (red) from eWAT. (**B**) MHCII expression in ATDCs in ND and HFD mice. (**C**) OTII- CD4$^+$ T cell proliferation after incubation with OVA-pulsed CD64$^+$ ATMs (middle) and CD11c$^+$CD64$^-$ ATDCs (right). One representative experiment from three independent replicates is shown. (**D**) ATDC subsets based on CD103, CD11b, CD4, CD8α, B220, and MHCII. (**E**) Quantitation of ATDC subsets in eWAT from ND- and HFD-fed C57 mice. (**F**) Quantitation of ATMs and ATDCs in lean WT and *Csf2*$^{-/-}$ mice. *$p < 0.05$, ***$p < 0.001$.

against the ImmGen core set of macrophage-specific genes (25), CD64$^+$ cells were significantly enriched for macrophage genes compared with CD64$^-$ cells both in lean and in obese mice (Fig. 2A). In contrast, expression of the core DC cell genes was highly enriched in CD64$^-$ cells compared with CD64$^+$ cells in both lean and obese conditions (Fig. 2B). Independent samples of FACS-sorted CD64$^+$ and CD64$^-$ cells from adipose tissue confirmed these differences (Fig. 2C). Core macrophage genes such as *Mertk* and *Camk1* were highly expressed in CD64$^+$ cells, whereas DC genes *Flt3* and *Zbtb46* were enriched in CD64$^-$CD11c$^+$ cells.

Gene Set Enrichment Analysis was used to identify uniquely enriched networks in ATDCs and CD11c$^+$ ATMs in obese mice (Fig. 2D). The top category for ATDCs was enrichment for genes involved in graft versus host disease and interactions between APCs and lymphoid cells. Examining this set showed that ATDCs are enriched for the expression of cytokine genes such as *Il2*, *Il1a*, *Ifng*, and *Il1b*, but not for *Il6* and *Tnfa* (Fig. 2E, 2F). We confirmed this by intracellular cytokine staining that showed a higher number of IL-6$^+$ and TNF-α$^+$ ATMs compared with ATDCs in lean and obese mice (Fig. 2G). For CD11c$^+$ ATMs, complement and coagulation cascade genes had the highest enrichment score along with genes involved in glycan biosynthesis and lysosomes. A lipid-laden phenotype with activated lysosomes is associated with obesity and seen in obese animals and human ATMs (33, 34). When ATMs and ATDCs from HFD-fed mice were examined for lipid accumulation by BODIPY staining, ATMs had significantly higher BODIPY staining compared with ATDCs (Fig. 2H).

ATDCs are predominantly CD11b$^+$ cDCs

The surface marker profile of CD45$^+$CD64$^-$CD11c$^+$ ATDCs was examined to further evaluate the phenotypes of ATDCs (Fig. 3A). Both ATMs and ATDCs from lean mice express MHCII, CD40, CD80, and CD86. All of these APC markers were expressed at higher levels in ATMs compared with ATDCs, which suggests an immature phenotype of ATDCs in lean mice. With obesity, MHCII expression in ATDCs was significantly increased (Fig. 3B). We have previously shown that ATMs are potent functional APCs. In vitro T cell stimulation assays were performed to compare ATM and ATDC APC function (Fig. 3C). CFSE-labeled CD4$^+$ T cells from OT-II mice were incubated with ATMs and ATDCs after loading with OVA (100 μg/ml). Both ATMs and ATDCs were able to stimulate T cell proliferation to a similar extent.

Additional markers were used to identify ATDC subpopulations (Fig. 3D). The majority of ATDCs in lean mice were CD11b$^+$ (>60%). Rare populations of CD103$^+$, B220$^+$, CD4$^+$, and CD8$^+$ ATDCs were also identified in lean mice, suggesting that the majority of ATDCs are of the conventional CD11b$^+$ type. In obese mice, CD11b$^+$ myeloid cDCs remained the dominant ATDC type, and the quantity of CD11b$^+$ conventional ATDCs (cATDCs) normalized to adipose tissue weight was increased by 2-fold compared with lean mice (Fig. 3E). There was a small but significant increase in CD8a$^+$CD11b$^-$ ATDCs with HFD, as well as a significant increase in ATDCs that were negative for CD103, CD8, or CD11b. Consistent with the prominence of myeloid-derived cATDCs (CD11b$^+$ DCs), ATDC content was decreased in *Csf2*$^{-/-}$ mice (Fig. 3F).

ATDCs are a dominant CD11c$^+$ population with moderate HFD exposure

We next performed time-course studies to examine the kinetics of accumulation of ATMs (CD11c$^+$ and CD11c$^-$) and ATDCs in gonadal/epididymal adipose tissue (eWAT; Fig. 4A). Mice were examined after 8 and 16 wk of HFD feeding. Sixteen weeks of HFD induced a significant increase in body weight associated with eWAT hypertrophy and the development of fasting hyperglycemia (data not shown). In lean mice, CD11c$^-$ ATMs were the dominant myeloid cell population as a percentage of all CD45$^+$ leukocytes and as a percentage of SVFs. The majority of CD11c$^+$ cells in lean mice were ATDCs and not ATMs. With 8 wk of HFD, both CD11c$^+$ ATMs and CD11c$^+$ ATDCs were increased to numbers that were similar to CD11c$^-$ ATMs. At this time point, ATDCs were still the dominant CD11c$^+$ cell in adipose tissue. Sixteen weeks of HFD exposure led to a substantial increase in CD11c$^+$ ATMs and the maintenance of a prominent population of ATDCs. In s.c./inguinal adipose tissue (iWAT), ATM content was not significantly increased with HFD feeding (Fig. 4B). However, there was a significant induction of ATDCs in iWAT similar to what is seen in eWAT.

Differential dependence of CD11c$^+$ ATMs and ATDCs on CCR2 during diet-induced obesity

Monocyte recruitment has been shown to be a primary mechanism by which CD11c$^+$ ATMs accumulate in adipose tissue in mice (32, 35). Because our results suggest that the prior definition of F4/80$^+$ CD11b$^+$CD11c$^+$ ATMs is contaminated with ATDCs and other leukocytes, we revisited ATM and ATDC accumulation in *Ccr2*$^{-/-}$

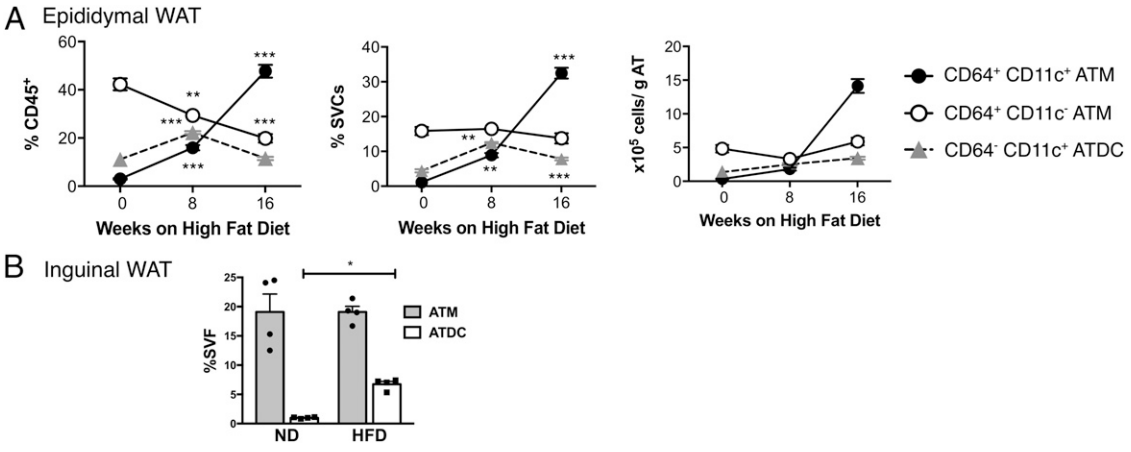

FIGURE 4. Time course of ATM and ATDC accumulation in adipose tissue with HFD-induced obesity. C57BL/6 male mice were fed an HFD for various time periods (0, 8, and 16 wk). (**A**) eWAT SVFs quantified for CD11c$^+$ ATMs, CD11c$^-$ ATMs, and ATDCs by flow cytometry normalized for adipose tissue mass. (**B**) Quantitation of ATMs and ATDCs in iWAT at 16 wk of HFD. *$p < 0.05$, **$p < 0.01$, ***$p < 0.001$.

mice using CD64. *Ccr2*$^{-/-}$ mice had significantly reduced ATMs and ATDCs compared with wild type (WT) (Fig. 5A). Specifically, CD11b^{+} ATDCs were decreased in *Ccr2*$^{-/-}$ mice, but there were no differences in CD11b^{-} ATDCs (Fig. 5B). With 2 wk of HFD, we observed an increase in ATDCs in WT, but not in *Ccr2*$^{-/-}$ mice, indicating that CCR2 is required for ATDC accumulation with short-term HFD exposure (Fig. 5C).

Because *Ccr2*$^{-/-}$ mice have fewer circulating monocytes (35), it is difficult to discern whether ATM and ATDC accumulation relies on *Ccr2*-dependent signals for monocyte trafficking or is dependent on the size of the monocyte pool. To evaluate this, we used a mixed chimera model where lethally irradiated recipients were reconstituted with a 1:1 mixture of bone marrow cells from WT (CD45.1) and *Ccr2*$^{-/-}$ (CD45.2) donor mice (Fig. 5D). After reconstitution, the chimeras were fed ND or HFD for 16 wk. Blood chimerism analysis was performed to evaluate the ratio of WT/*Ccr2*$^{-/-}$ cells (CD45.1/CD45.2) relative to the bone marrow input ratio of 1. Analysis of total peripheral blood leukocytes demonstrated a slight bias toward reconstitution with cells from *Ccr2*$^{-/-}$ donors with the ratio of WT/*Ccr2*$^{-/-}$ cells (CD45.1/CD45.2) <1 in both ND and HFD conditions. However, analysis of circulating CD115^{+} monocytes demonstrated a significant increase in monocytes derived from WT compared with *Ccr2*$^{-/-}$ mice with a WT/*Ccr2*$^{-/-}$ ratio of 11.3 $\pm$ 1.6 (Fig. 5E). Circulating WT-derived cells dominated over *Ccr2*$^{-/-}$ cells in both Ly-6c^{hi} and Ly-6c^{lo} monocyte subsets. This is consistent with the

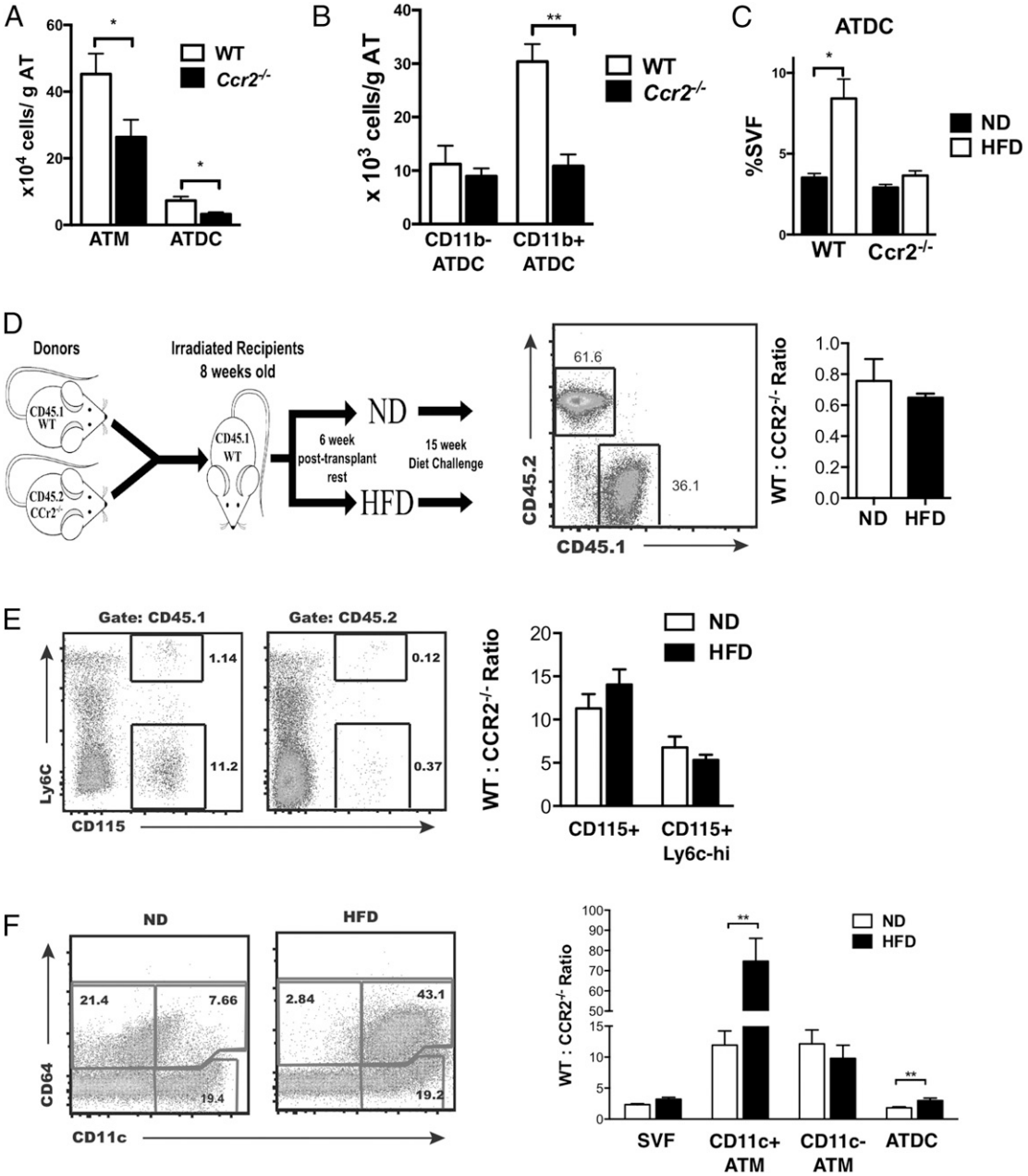

FIGURE 5. CCR2 is required for obesity-induced CD11c^{+} ATM and ATDC migration into adipose tissue. (**A**) Quantitation of CD11c^{+} ATMs, CD11c^{-} ATMs, and ATDCs in eWAT from WT and *Ccr2*$^{-/-}$ mice. (**B**) Quantitation of CD11b^{+} and CD11b^{-} ATDC subsets in eWAT from WT and *Ccr2*$^{-/-}$ mice. (**C**) ATM and ATDC content in WT and *Ccr2*$^{-/-}$ mice after 2 wk of ND or HFD feeding. (**D**) Diagram of mixed chimera experiment design. *Ccr2*$^{-/-}$ (CD45.2) and WT (CD45.1) bone marrow mixed in a 1:1 ratio before injection in irradiated recipients. Chimerism analysis of blood leukocytes is shown. (**E**) Frequency and ratio of CD45.1 (WT) and CD45.2 (*Ccr2*$^{-/-}$) in blood monocytes from lean and obese (15-wk HFD) chimeric mice. (**F**) Frequency and CD45.1/CD45.2 ratio in CD11c^{+} ATMs, CD11c^{-} ATMs, and ATDCs in eWAT. *$p < 0.05$, **$p < 0.01$ versus ND.

requirement of CCR2 to regulate monocyte exit from the bone marrow compartment into the circulation.

ATMs in eWAT were examined in the chimeras (Fig. 5F). As expected, CD64$^+$ ATMs from ND-fed mice were primarily CD11c$^-$, whereas HFD induced CD11c$^+$ ATM accumulation. In lean mice, the WT/*Ccr2*$^{-/-}$ ratio in both CD11c$^-$ and CD11c$^+$ ATMs was elevated (12.2 $\pm$ 2.2 and 11.9 $\pm$ 2.2, respectively) and was similar to what was observed in blood monocytes. This suggests that in a competitive reconstitution model both ATM subsets in lean mice may be dependent on circulating monocyte for reconstitution. In contrast, the WT/*Ccr2*$^{-/-}$ ratio of ATDCs in lean mice was significantly lower (1.8 $\pm$ 0.16) than what was observed in either ATM or circulating monocytes. In obese mice, the WT/*Ccr2*$^{-/-}$ ratio of CD11c$^+$ ATMs was markedly increased (74.7 $\pm$ 11.7) compared with lean mice. This demonstrates that, in the obese environment, WT monocytes had a significant competitive advantage in trafficking to adipose tissue from the circulation compared with *Ccr2*$^{-/-}$ monocytes. In contrast, there was no change in the WT/*Ccr2*$^{-/-}$ ratio of CD11c$^-$ ATMs, suggesting that any accumulation of CD11c$^-$ ATMs during obesity is CCR2 independent. Although the WT/*Ccr2*$^{-/-}$ ratio of ATDCs was lower than that of monocytes in lean mice, there was a statistically significant increase in the WT/*Ccr2*$^{-/-}$ ratio in ATDCs (3.0 $\pm$ 0.4) in obese mice, suggesting some ATDCs are dependent on CCR2 for trafficking to adipose tissue with obesity and consistent with analysis of *Ccr2*$^{-/-}$ mice. However, the CCR2-dependent induction of ATDCs during obesity was less efficient than that of CD11c$^+$ ATMs (~1.6-fold in ATDC versus ~6.3-fold in CD11c$^+$ ATMs). Overall, this suggests that in chronic obesity, CCR2 signaling plays a critical role in regulating monocyte trafficking into obese adipose tissue to generate CD11c$^+$ ATMs and ATDCs.

CCR7 is required for the HFD-induced ATDC accumulation and insulin resistance

The microarray analysis identified *Ccr7* as differentially expressed in ATDCs compared with ATMs. To evaluate whether CCR7 plays a role in the recruitment or maintenance of ATDC in adipose tissue, we fed age-matched male WT and *Ccr7*$^{-/-}$ mice ND or HFD ad libitum for 8 wk. This feeding duration was chosen based on our observation that 8 wk led to increased ATDCs but minimal accumulation of CD11c$^+$ ATMs. In ND-fed mice, the quantity of CD11c$^+$ and CD11c$^-$ ATMs did not differ between genotypes. However, *Ccr7*$^{-/-}$ mice had significantly fewer ATDCs compared with WT mice primarily because of a decrease in CD11b$^+$ ATDCs (Fig. 6A, 6B). Eight-week HFD challenge induced CD11c$^+$ ATM and ATDC accumulation in both genotypes, but HFD-induced ATDC accumulation was significantly impaired in *Ccr7*$^{-/-}$ mice when normalized to adipose tissue weight (Fig. 6C). CD11b$^+$ ATDCs in *Ccr7*$^{-/-}$ adipose tissue were ~50% lower than WT adipose tissue whereas the quantity of CD11b$^-$ ATDCs was similar between genotypes (Fig. 6D). After 8 wk of HFD, *Ccr7*$^{-/-}$ mice had normal numbers of circulating monocytes and similar levels of Ly-6C^{hi} and Ly6C^{lo} monocytes compared with WT

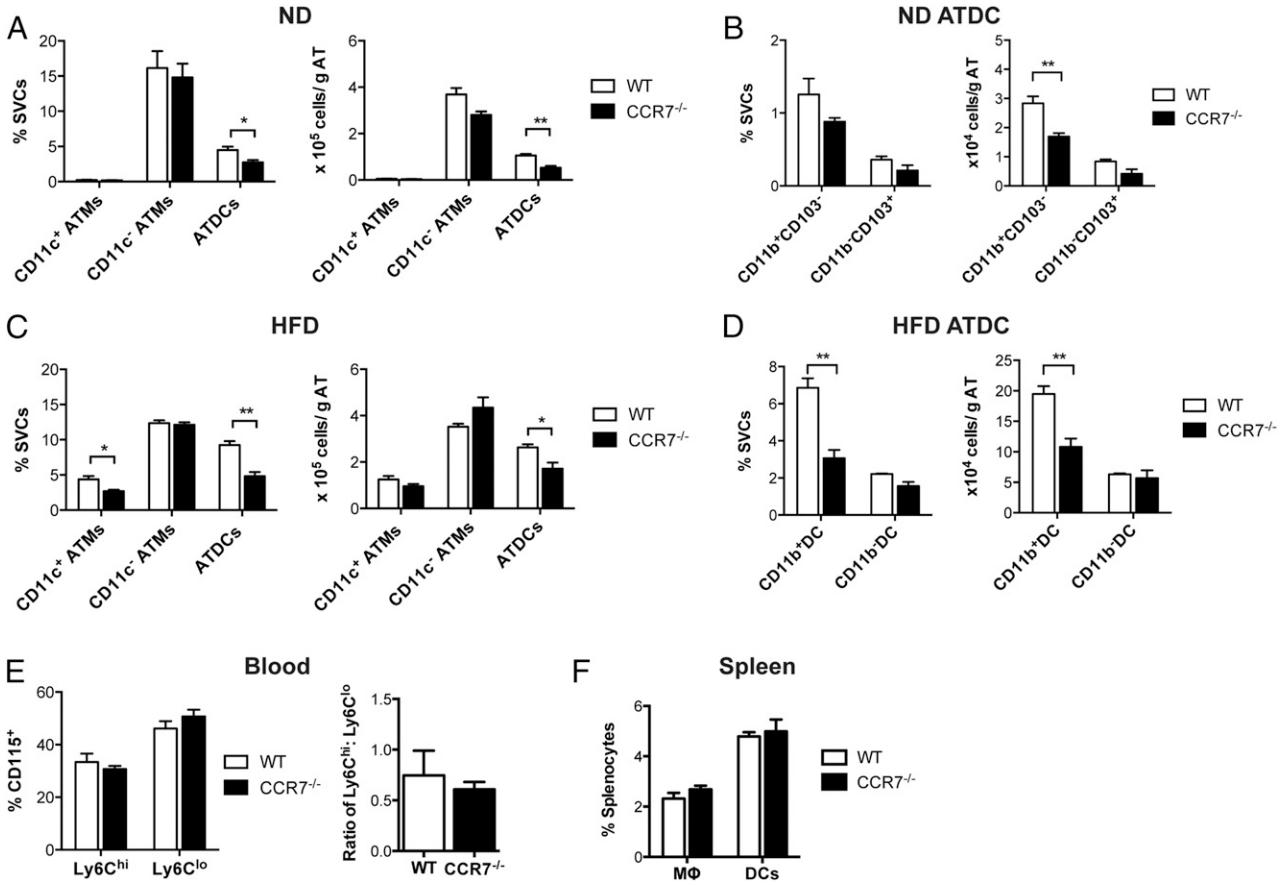

FIGURE 6. CCR7 is required for ATDC accumulation during diet-induced obesity. (**A**) Quantitation of ATMs and ATDCs in eWAT from chow-fed WT and *Ccr7*$^{-/-}$ mice. (**B**) Quantitation of CD11b$^+$CD103$^-$ and CD11b$^-$ CD103$^+$ ATDC subsets in eWAT from WT and *Ccr7*$^{-/-}$ mice. (**C**) Quantitation of CD11c$^+$ ATMs, CD11c$^-$ ATMs, and ATDCs in eWAT from WT and *Ccr7*$^{-/-}$ mice fed HFD for 8 wk. (**D**) Quantitation of CD11b$^+$ and CD11b$^-$ ATDC subsets in eWAT from WT and *Ccr7*$^{-/-}$ HFD-fed mice. (**E**) Frequency of Ly6^{hi} and Ly6^{lo} blood monocytes from WT and *Ccr7*$^{-/-}$ mice. (**F**) Frequency of macrophages and DCs in spleen from WT and *Ccr7*$^{-/-}$. *$p < 0.05$, **$p < 0.01$.

(Fig. 6E). Importantly, there was no difference in the accumulation of splenic macrophages and DCs between genotypes (Fig. 6F). These data suggest that HFD induces ATDC accumulation via CCR7-dependent increases in CD11b$^+$ ATDCs.

We next examined the impact of *Ccr7* deficiency on HFD-induced insulin resistance and adipose tissue inflammation. Total body weight between the genotypes was not significantly different on HFD (Fig. 7A). *Ccr7*$^{-/-}$ mice had lower eWAT weights (Fig. 7B). iWAT and liver weight were similar between genotypes. Compared with WT mice, *Ccr7*$^{-/-}$ mice had lower fasting glucose levels and fasting insulin levels, resulting in an improvement in insulin sensitivity in *Ccr7*$^{-/-}$ mice based on the calculation of HOMA-IR (Fig. 7C, 7D). Whole-mount imaging of eWAT showed a significant accumulation of Mac2$^+$ in CLS in WT eWAT, whereas CLS were largely absent in *Ccr7*$^{-/-}$ eWAT (Fig. 7E). Consistent with the flow cytometry data, gene expression of *Itgax* and *Flt3* were decreased in *Ccr7*$^{-/-}$ eWAT. In addition, *Ccl2* and *IL-6* expression were decreased and *Foxp3* expression was increased in *Ccr7*$^{-/-}$ eWAT (Fig. 7F). Obese *Ccr7*$^{-/-}$ mice had an increase in adipose tissue CD4$^+$ and CD8$^+$ cells, suggesting that a lack of T cells does not explain metabolic protection in these mice (data not shown). Overall, these data suggest that CCR7-dependent signals contribute to insulin resistance and adipose tissue inflammation by regulating ATDC content independent of ATM.

CD64$^-$ ATDCs are enriched in s.c. adipose tissue from obese humans

A range of markers has been used to quantify human ATM in published studies, and many rely on CD14 as an ATM marker despite the demonstration of CD14$^+$ DCs (36). We therefore wanted to evaluate the utility of CD64 in delineating ATMs from ATDCs in human samples. Multicolor flow cytometry was performed on SVF cells from s.c. and omental/visceral adipose tissue (OM) from obese subjects undergoing bariatric surgery. Using CD64, we identified a major population of CD45$^+$CD11b$^+$CD64$^+$ cells with minor populations of CD45$^+$CD11b$^+$CD64$^-$ and CD45$^+$CD11b$^-$CD64$^+$ cells (Fig. 8A). CD45$^+$CD11b$^+$CD64$^+$ stained uniformly positive for CD14$^+$. However, a minor population of CD14$^+$ cells was observed in the CD45$^+$CD11b$^+$CD64$^-$ and CD45$^+$CD11b$^-$CD64$^+$ populations. Using CD64 and CD11c, we identified CD64$^+$CD11c$^+$, CD64$^+$CD11c$^-$, and CD64$^-$CD11c$^+$ myeloid leukocyte populations (Fig. 8B). All three populations expressed CD1c and HLA-DR. However, CD45$^+$CD64$^-$CD11c$^+$ cells had the highest CD1c expression and moderate HLA-DR expression compared with the CD45$^+$CD64$^+$ population. CD206 was primarily expressed on CD64$^+$CD11c$^-$ cells, consistent with mouse studies suggesting this is the phenotype of resident ATMs. CD64$^+$ cells were CD16$^-$ in human adipose tissue, and CD64$^-$CD16$^+$ cells were a mix of monocytes and neutrophils based on side

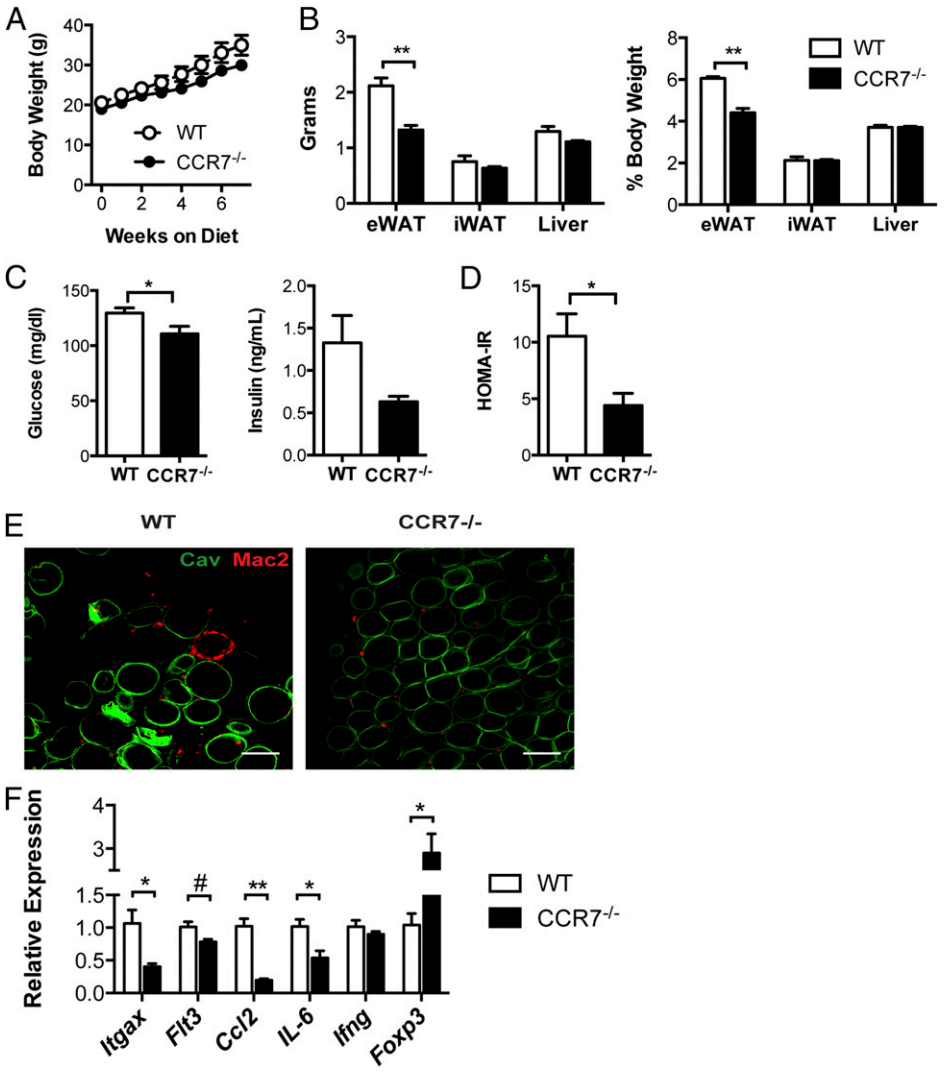

FIGURE 7. CCR7-deficient mice are protected from HFD-induced insulin resistance and adipose tissue inflammation. (**A**) Body weights of WT and *Ccr7*$^{-/-}$ mice during 8-wk HFD feeding. (**B**) Organ weights at the end of HFD exposure. (**C**) Fasting blood glucose and plasma insulin levels. (**D**) HOMA-IR in WT and *Ccr7*$^{-/-}$ mice fed HFD for 8 wk. (**E**) Immunofluorescence imaging of Mac2$^+$ ATM (red) and caveolin$^+$ adipocytes (green) in eWAT. Scale bar, 100 μm. (**F**) Expression of inflammatory genes in eWAT from HFD-fed WT and *Ccr7*$^{-/-}$ mice. $^*p < 0.05$, $^{**}p < 0.01$, $^{\#}p = 0.06$.

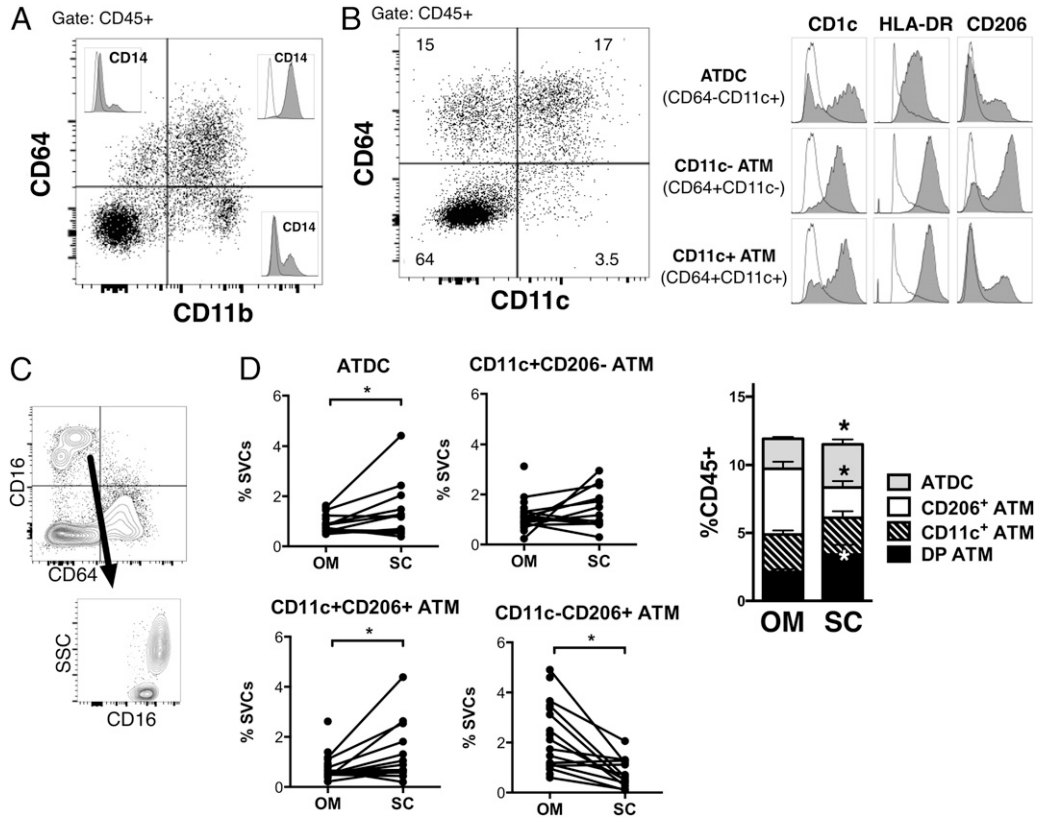

FIGURE 8. $CD64^-$ $CD11c^+$ ATDCs are enriched in s.c. adipose tissue in obese humans. (**A**) SVFs were isolated from human omental (OM) and s.c. adipose tissue, and analyzed by flow cytometry. Analysis of CD64-expressing cells and overlap with CD14 in OM. A representative plot of three independent experiments is shown. (**B**) Marker expression of $CD64^-$ $CD11c^+$ ATDCs, $CD64^+$ $CD11c^-$ ATMs, and $CD64^+$ $CD11c^+$ ATMs in OM. (**C**) Contour plot showing CD16 and CD64. (**D**) Frequency of ATDCs, $CD11c^+CD206^-$ ATMs, $CD11c^+CD206^+$ ATMs, and $CD11c^-CD206^+$ ATMs in paired OM and s.c. adipose tissue from obese patients (n = 10–14). $*p < 0.05$ versus OM.

scatter (Fig. 8C). Overall, this suggests that human ATDCs can be defined as $CD64^-CD11c^+$ as in mice.

We next examined the proportion of ATDC ($CD64^-$) and ATM ($CD64^+$) subsets in paired samples from s.c. and OM depots (Fig. 8D). $CD11c^+CD206^+$ ATMs were enriched in s.c. compared with OM adipose tissue, whereas $CD11c^-CD206^+$ ATMs were lower in s.c. adipose tissue. The frequency of ATDCs was higher in s.c. compared with OM adipose tissue. Collectively, these results indicate that ATDCs are enriched in s.c. adipose tissue in obese humans.

Discussion

There is considerable interest in the contribution of myeloid cells including neutrophils, monocytes, macrophages, and DCs to obesity-induced inflammation and metabolic disease pathogenesis. Because the adipose tissue leukocyte network is unique, the goal of this study was to clearly and definitively delineate ATMs from ATDCs and examine their regulation with obesity. By using CD64 as a specific macrophage marker, our primary findings suggest that defining ATM as $F4/80^+CD11b^+$ leukocytes does not fully exclude other leukocyte types. More importantly, the $F4/80^+CD11b^+$ $CD11c^+$ cell subset can be contaminated with a distinct ATDC population that comprises a significant population of the total myeloid network in adipose tissue. ATDCs are primarily myeloid ($CD11b^+$) cDCs and accumulate with obesity. However, ATDC accumulation appears to be regulated by different chemotactic cues compared with ATM. In particular, ATDCs are CCR7 dependent and $Ccr7^{-/-}$ mice with lower ATDC content are protected from obesity-induced inflammation and insulin resistance.

ATMs have been defined almost exclusively using the markers $F4/80^+CD11b^+$ by our group and others (8, 34, 37). Our experiments suggest that some studies may need to be reevaluated and that changes in the $F4/80^+CD11b^+CD11c^+$ ATM may be accounted for by changes in ATDC quantity. In addition, our experiments suggest that the use of CD11c as a single marker to define ATDCs, which has been used by some groups, is inadequate given the clear identification of $CD11c^+$ ATMs particularly in obese mice (21). Care must also be taken with studies that use *LysM*-Cre recombinase because this may also target ATDCs (38). Our studies agree with the results of the ImmGen Consortium supporting the specificity of CD64 as a marker of tissue macrophages (22, 25). In addition, we have extended their results to the study of obese mouse models and obese human adipose tissue and support the specificity of CD64 as a marker of ATM in both contexts.

Our observation that ATDCs increase with early obesity and are the dominant $CD11c^+$ cells in adipose tissue with moderate HFD may be important to the control of adaptive immunity. Eight weeks of HFD correlates with alterations in adaptive immunity including changes in CD8 and CD4 adipose tissue T cell populations (39–41). $Ccr7^{-/-}$ mice with fewer ATDCs showed metabolic improvement at 8 wk of HFD, suggesting that ATDC signals may be important at the early stages of obesity. Lack of CD4 or CD8 T cells in adipose tissue did not explain this observation, although we cannot rule out other factors such as microbiome differences that may explain these differences. This suggests that ATDCs and ATMs independently contribute to directing adaptive immune responses induced by obesity because

both populations are potent APCs (15, 16). Ablation of CD11c$^+$ cells improves glucose intolerance partially by deactivating conventional T cells in adipose tissue (16). Whether this is due to alterations in ATMs, ATDCs, or both will have to be examined in future studies. We have previously shown that ATMs are required for T cell activation using *LysM*-Cre mice, but the results from this study indicate that we cannot eliminate the possibility of ATDC contribution for this effect.

Our observation of protection from insulin resistance in *Ccr7*$^{-/-}$ mice agrees with recent reports and identifies loss of the ATDC population as a primary mechanism for this effect (42). *CCR7* was identified in a module of signal transduction genes that were downregulated with weight loss after bariatric surgery that was disconnected from T cell signaling genes (43). The functional profile of ATDCs in the setting of obesity is strikingly different from that of CD11c$^+$ ATMs. Unlike ATMs, lysosomal and lipid storage are not induced in ATDCs with obesity. Instead, pathways related to Ag presentation and cytokine signaling remain elevated in ATDCs, suggesting that they have an independent contribution to the adipose tissue immune activation environment.

The protective effect of *Ccr2* deficiency in adipose tissue inflammation has been supported by several studies (35, 44, 45). However, separating the defects in circulating monocytes in *Ccr2*$^{-/-}$ mice from the defects in migration into peripheral tissues in this model is a challenge (46). Our competitive bone marrow experiments demonstrate that *Ccr2*$^{+/+}$ monocytes have an advantage for recruitment from the circulation into adipose tissue compared with *Ccr2*$^{-/-}$ monocytes independent of effects on the quantity of circulating monocytes. This supports the regulation of CD11c$^+$ ATMs by CCR2-dependent mechanisms and suggests that some cATDCs are recruited to adipose tissue by CCR2-dependent mechanisms. However, the CCR2 dependency was much lower for ATDC recruitment, compared with ATM, and suggests that ATDCs are likely not monocyte derived. Thus, ATDCs may not be monocyte derived and may instead be dependent on pre-DC populations from the circulation.

Overall, our studies clarify the somewhat confusing literature on CD11c expression in adipose tissue myeloid cells. We propose that there are three primary myeloid cell populations in adipose tissue: resident CD45$^+$CD64$^+$CD11c$^-$ ATMs, recruited CD45$^+$CD64$^+$CD11c$^+$ ATMs, and CD45$^+$CD64$^-$CD11c$^+$ ATDCs that are predominantly CD11b$^+$ cATDCs. Importantly, these observations extend to human adipose tissue and help inform future studies. ATDCs are not a minor population and can be as numerous as ATM subsets depending on the depot. The elevated levels of ATDC in human s. c. adipose tissue may explain the lower inflammatory capacity of this depot. Whether s.c. ATDCs are similar in function as OM ATDCs will be examined in future studies. An additional limitation is the lack of samples from lean individuals for comparison that is the topic of ongoing studies in our group. Clarifying the landscape of functional APCs in adipose tissue may also advance our understanding of the mechanisms by which regulatory and conventional adaptive immunity is controlled in adipose tissue where resident T cells appear to have unique properties compared with other nonlymphoid tissues (17).

Disclosures

The authors have no financial conflicts of interest.

References

1. Mathis, D. 2013. Immunological goings-on in visceral adipose tissue. *Cell Metab.* 17: 851–859.
2. Lumeng, C. N., and A. R. Saltiel. 2011. Inflammatory links between obesity and metabolic disease. *J. Clin. Invest.* 121: 2111–2117.
3. Lumeng, C. N. 2013. Innate immune activation in obesity. *Mol. Aspects Med.* 34: 12–29.
4. Skinner, A. C., M. J. Steiner, F. W. Henderson, and E. M. Perrin. 2010. Multiple markers of inflammation and weight status: cross-sectional analyses throughout childhood. *Pediatrics* 125: e801–e809.
5. Poitou, C., E. Dalmas, M. Renovato, V. Benhamo, F. Hajduch, M. Abdennour, J. F. Kahn, N. Veyrie, S. Rizkalla, W. H. Fridman, et al. 2011. CD14dimCD16+ and CD14+CD16+ monocytes in obesity and during weight loss: relationships with fat mass and subclinical atherosclerosis. *Arterioscler. Thromb. Vasc. Biol.* 31: 2322–2330.
6. Wentworth, J. M., G. Naselli, W. A. Brown, L. Doyle, B. Phipson, G. K. Smyth M. Wabitsch, P. E. O'Brien, and L. C. Harrison. 2010. Pro-inflammatory CD11c+CD206+ adipose tissue macrophages are associated with insulin resistance in human obesity. *Diabetes* 59: 1648–1656.
7. Talukdar, S., D. Y. Oh, G. Bandyopadhyay, D. Li, J. Xu, J. McNelis, M. Lu, P. Li, Q. Yan, Y. Zhu, et al. 2012. Neutrophils mediate insulin resistance in mice fed a high-fat diet through secreted elastase. *Nat. Med.* 18: 1407–1412.
8. Lumeng, C. N., J. L. Bodzin, and A. R. Saltiel. 2007. Obesity induces a phenotypic switch in adipose tissue macrophage polarization. *J. Clin. Invest.* 117: 175–184.
9. Lumeng, C. N., J. B. DelProposto, D. J. Westcott, and A. R. Saltiel. 2008. Phenotypic switching of adipose tissue macrophages with obesity is generated by spatiotemporal differences in macrophage subtypes. *Diabetes* 57: 3239–3246.
10. Xu, X., A. Grijalva, A. Skowronski, M. van Eijk, M. J. Serlie, and A. W. Ferrante, Jr. 2013. Obesity activates a program of lysosomal-dependent lipid metabolism in adipose tissue macrophages independently of classic activation. *Cell Metab.* 18: 816–830.
11. Kratz, M., B. R. Coats, K. B. Hisert, D. Hagman, V. Mutskov, E. Peris, K. Q. Schoenfelt, J. N. Kuzma, I. Larson, P. S. Billing, et al. 2014. Metabolic dysfunction drives a mechanistically distinct proinflammatory phenotype in adipose tissue macrophages. *Cell Metab.* 20: 614–625.
12. Wu, H., X. D. Perrard, Q. Wang, J. L. Perrard, V. R. Polsani, P. H. Jones, C. W. Smith, and C. M. Ballantyne. 2010. CD11c expression in adipose tissue and blood and its role in diet-induced obesity. *Arterioscler. Thromb. Vasc. Biol.* 30: 186–192.
13. Tao, T., S. Li, A. Zhao, Y. Zhang, and W. Liu. 2012. Expression of the CD11c gene in subcutaneous adipose tissue is associated with cytokine level and insulin resistance in women with polycystic ovary syndrome. *Eur. J. Endocrinol.* 167: 705–713.
14. Wu, H., R. M. Gower, H. Wang, X. Y. Perrard, R. Ma, D. C. Bullard, A. R. Burns, A. Paul, C. W. Smith, S. I. Simon, and C. M. Ballantyne. 2009. Functional role of CD11c+ monocytes in atherogenesis associated with hypercholesterolemia. *Circulation* 119: 2708–2717.
15. Patsouris, D., P. P. Li, D. Thapar, J. Chapman, J. M. Olefsky, and J. G. Neels. 2008. Ablation of CD11c-positive cells normalizes insulin sensitivity in obese insulin resistant animals. *Cell Metab.* 8: 301–309.
16. Cho, K. W., D. L. Morris, J. L. DelProposto, L. Geletka, B. Zamarron, G. Martinez-Santibanez, K. A. Meyer, K. Singer, R. W. O'Rourke, and C. N. Lumeng. 2014. An MHC II-dependent activation loop between adipose tissue macrophages and CD4+ T cells controls obesity-induced inflammation. *Cell Reports* 9: 605–617.
17. Kolodin, D., N. van Panhuys, C. Li, A. M. Magnuson, D. Cipolletta, C. M. Miller, A. Wagers, R. N. Germain, C. Benoist, and D. Mathis. 2015. Antigen- and cytokine-driven accumulation of regulatory T cells in visceral adipose tissue of lean mice. *Cell Metab.* 21: 543–557.
18. Morris, D. L., K. W. Cho, J. L. Delproposto, K. E. Oatmen, L. M. Geletka, G. Martinez-Santibanez, K. Singer, and C. N. Lumeng. 2013. Adipose tissue macrophages function as antigen-presenting cells and regulate adipose tissue CD4+ T cells in mice. *Diabetes* 62: 2762–2772.
19. Bertola, A., T. Ciucci, D. Rousseau, V. Bourlier, C. Duffaut, S. Bonnafous, C. Blin-Wakkach, R. Anty, A. Iannelli, J. Gugenheim, et al. 2012. Identification of adipose tissue dendritic cells correlated with obesity-associated insulin-resistance and inducing Th17 responses in mice and patients. *Diabetes* 61: 2238–2247.
20. Stefanovic-Racic, M., X. Yang, M. S. Turner, B. S. Mantell, D. B. Stolz, T. L. Sumpter, I. J. Sipula, N. Dedousis, D. K. Scott, P. A. Morel, et al. 2012. Dendritic cells promote macrophage infiltration and comprise a substantial proportion of obesity-associated increases in CD11c+ cells in adipose tissue and liver. *Diabetes* 61: 2330–2339.
21. Chen, Y., J. Tian, X. Tian, X. Tang, K. Rui, J. Tong, L. Lu, H. Xu, and S. Wang. 2014. Adipose tissue dendritic cells enhances inflammation by prompting the generation of Th17 cells. *PLoS One* 9: e92450.
22. Kuan, E. L., S. Ivanov, E. A. Bridenbaugh, G. Victora, W. Wang, E. W. Childs, A. M. Platt, C. V. Jakubzick, R. J. Mason, A. A. Gashev, et al. 2015. Collecting lymphatic vessel permeability facilitates adipose tissue inflammation and distribution of antigen to lymph node-homing adipose tissue dendritic cells. *J. Immunol.* 194: 5200–5210.
23. Zlotnikov-Klionsky, Y., B. Nathansohn-Levi, E. Shezen, C. Rosen, S. Kagan, L. Bar-On, S. Jung, E. Shifrut, S. Reich-Zeliger, N. Friedman, et al. 2015. Perforin-positive dendritic cells exhibit an immuno-regulatory role in metabolic syndrome and autoimmunity. *Immunity* 43: 776–787.
24. Pamir, N., N. C. Liu, A. Irwin, L. Becker, Y. Peng, G. E. Ronsein, K. E. Bornfeldt, J. S. Duffield, and J. W. Heinecke. 2015. Granulocyte/macrophage colony-stimulating factor-dependent dendritic cells restrain lean adipose tissue expansion. *J. Biol. Chem.* 290: 14656–14667.
25. Gautier, E. L., T. Shay, J. Miller, M. Greter, C. Jakubzick, S. Ivanov, J. Helft, A. Chow, K. G. Elpek, S. Gordonov, et al; Immunological Genome Consortium.

2012. Gene-expression profiles and transcriptional regulatory pathways that underlie the identity and diversity of mouse tissue macrophages. *Nat. Immunol.* 13: 1118–1128.
26. Tamoutounour, S., S. Henri, H. Lelouard, B. de Bovis, C. de Haar, C. J. van der Woude, A. M. Woltman, Y. Reyal, D. Bonnet, D. Sichien, et al. 2012. CD64 distinguishes macrophages from dendritic cells in the gut and reveals the Th1-inducing role of mesenteric lymph node macrophages during colitis. *Eur. J. Immunol.* 42: 3150–3166.
27. De Calisto, J., E. J. Villablanca, and J. R. Mora. 2012. FcγRI (CD64): an identity card for intestinal macrophages. *Eur. J. Immunol.* 42: 3136–3140.
28. Singer, K., J. DelProposto, D. L. Morris, B. Zamarron, T. Mergian, N. Maley, K. W. Cho, L. Geletka, P. Subbaiah, L. Muir, et al. 2014. Diet-induced obesity promotes myelopoiesis in hematopoietic stem cells. *Mol. Metab.* 3: 664–675.
29. Martinez-Santibañez, G., K. W. Cho, and C. N. Lumeng. 2014. Imaging white adipose tissue with confocal microscopy. *Methods Enzymol.* 537: 17–30.
30. Cho, K. W., D. L. Morris, and C. N. Lumeng. 2014. Flow cytometry analyses of adipose tissue macrophages. *Methods Enzymol.* 537: 297–314.
31. Lumeng, C. N., S. M. Deyoung, J. L. Bodzin, and A. R. Saltiel. 2007. Increased inflammatory properties of adipose tissue macrophages recruited during diet-induced obesity. *Diabetes* 56: 16–23.
32. Westcott, D. J., J. B. Delproposto, L. M. Geletka, T. Wang, K. Singer, A. R. Saltiel, and C. N. Lumeng. 2009. MGL1 promotes adipose tissue inflammation and insulin resistance by regulating 7/4hi monocytes in obesity. *J. Exp. Med.* 206: 3143–3156.
33. Shapiro, H., T. Pecht, R. Shaco-Levy, I. Harman-Boehm, B. Kirshtein, Y. Kuperman, A. Chen, M. Blüher, I. Shai, and A. Rudich. 2013. Adipose tissue foam cells are present in human obesity. *J. Clin. Endocrinol. Metab.* 98: 1173–1181.
34. Kosteli, A., E. Sugaru, G. Haemmerle, J. F. Martin, J. Lei, R. Zechner, and A. W. Ferrante, Jr. 2010. Weight loss and lipolysis promote a dynamic immune response in murine adipose tissue. *J. Clin. Invest.* 120: 3466–3479.
35. Weisberg, S. P., D. Hunter, R. Huber, J. Lemieux, S. Slaymaker, K. Vaddi, I. Charo, R. L. Leibel, and A. W. Ferrante, Jr. 2006. CCR2 modulates inflammatory and metabolic effects of high-fat feeding. *J. Clin. Invest.* 116: 115–124.
36. Collin, M., N. McGovern, and M. Haniffa. 2013. Human dendritic cell subsets. *Immunology* 140: 22–30.
37. Orr, J. S., M. J. Puglisi, K. L. Ellacott, C. N. Lumeng, D. H. Wasserman, and A. H. Hasty. 2012. Toll-like receptor 4 deficiency promotes the alternative activation of adipose tissue macrophages. *Diabetes* 61: 2718–2727.
38. Jakubzick, C., M. Bogunovic, A. J. Bonito, E. L. Kuan, M. Merad, and G. J. Randolph. 2008. Lymph-migrating, tissue-derived dendritic cells are minor constituents within steady-state lymph nodes. *J. Exp. Med.* 205: 2839–2850.
39. Winer, S., Y. Chan, G. Paltser, D. Truong, H. Tsui, J. Bahrami, R. Dorfman, Y. Wang, J. Zielenski, F. Mastronardi, et al. 2009. Normalization of obesity-associated insulin resistance through immunotherapy. *Nat. Med.* 15: 921–929.
40. Feuerer, M., L. Herrero, D. Cipolletta, A. Naaz, J. Wong, A. Nayer, J. Lee, A. B. Goldfine, C. Benoist, S. Shoelson, and D. Mathis. 2009. Lean, but not obese, fat is enriched for a unique population of regulatory T cells that affect metabolic parameters. *Nat. Med.* 15: 930–939.
41. Nishimura, S., I. Manabe, M. Nagasaki, K. Eto, H. Yamashita, M. Ohsugi, M. Otsu, K. Hara, K. Ueki, S. Sugiura, et al. 2009. CD8+ effector T cells contribute to macrophage recruitment and adipose tissue inflammation in obesity. *Nat. Med.* 15: 914–920.
42. Sano, T., M. Iwashita, S. Nagayasu, A. Yamashita, T. Shinjo, A. Hashikata, T. Asano, A. Kushiyama, N. Ishimaru, Y. Takahama, and F. Nishimura. 2015. Protection from diet-induced obesity and insulin resistance in mice lacking CCL19-CCR7 signaling. *Obesity (Silver Spring)* 23: 1460–1471.
43. Poitou, C., C. Perret, F. Mathieu, V. Truong, Y. Blum, H. Durand, R. Alili, N. Chelghoum, V. Pelloux, J. Aron-Wisnewsky, et al. 2015. Bariatric surgery induces disruption in inflammatory signaling pathways mediated by immune cells in adipose tissue: a RNA-seq study. *PLoS One* 10: e0125718.
44. Kang, Y. S., J. J. Cha, Y. Y. Hyun, and D. R. Cha. 2011. Novel C-C chemokine receptor 2 antagonists in metabolic disease: a review of recent developments. *Expert Opin. Investig. Drugs* 20: 745–756.
45. Obstfeld, A. E., E. Sugaru, M. Thearle, A. M. Francisco, C. Gayet, H. N. Ginsberg, E. V. Ables, and A. W. Ferrante, Jr. 2010. C-C chemokine receptor 2 (CCR2) regulates the hepatic recruitment of myeloid cells that promote obesity-induced hepatic steatosis. *Diabetes* 59: 916–925.
46. Tacke, F., D. Alvarez, T. J. Kaplan, C. Jakubzick, R. Spanbroek, J. Llodra, A. Garin, J. Liu, M. Mack, N. van Rooijen, et al. 2007. Monocyte subsets differentially employ CCR2, CCR5, and CX3CR1 to accumulate within atherosclerotic plaques. *J. Clin. Invest.* 117: 185–194.

Supplemental Table 1. Flow cytometry antibodies used in this study

Antibody	Clone	Company
Anti-mouse		
CD11b	M1/70	eBioscience
CD11c	N418	eBioscience
CD45.2	104	eBioscience
CD45.1	A20	eBioscience
CD64	X54-5/7.1	BD Biosciences
MHC I-A/I-E	M5/114.15.2	eBioscience
F4/80	BM8	eBioscience
CD206	MR5D3	AbD Serotec
Siglec-F	E50-2440	BD Biosciences
Ly6G	RB6-8C5	eBioscience
CD40	1C10	eBioscience
CD80	16-10A1	eBioscience
CD86	GL1	eBioscience
CD103	2E7	eBioscience
CD4	RM4-5	eBioscience
CD8a	53-6.7	eBioscience
B220	RA3-6B2	eBioscience
CD115	AFS98	eBioscience
Ly6C	AL21	BD Biosciences
Anti-human		
CD206	15-2	Biolegend
CD11c	3.9	Biolegend
CD11b	44	BD Biosciences
CD14	RMO52	Beckman
CD45	HI30	eBioscience
CD1c	F10/21A3	BD Bioscience
CD64	10.1	eBioscience

Supplemental Table 2. Sequences for RT-PCR primers used in this study

Gene	Primer	Sequence
Arbp	Forward	AGA TTC GGG ATA TGC TGT TGG C
	Reverse	TCG GGT CCT AGA CCA GTG TTC
18S	Forward	TTG ACG GAA GGG CAC CAC CAG
	Reverse	GCA CCA CCA CCC ACG GAA TCG
Flt3	Forward	GAG CGA CTC CAG CTA CGT C
	Reverse	ACC CAG TGA AAA TAT CTC CCA GA
Mertk	Forward	CAG GGC CTT TAC CAG GGA GA
	Reverse	TGT GTG CTG GAT GTG ATC TTC
Camk1	Forward	AAG CAG GCG GAA GAC ATT AGG
	Reverse	AGT TTC TGA GTC CTC TTG TCC T
Zbtb46	Forward	AGA GAG CAC ATG AAG CGA CA
	Reverse	CTG GCT GCA GAC ATG AAC AC
Fcgr1	Forward	AGG TTC CTC AAT GCC AAG TGA
	Reverse	GCG ACC TCC GAA TCT GAA GA
kit	Forward	GCC ACG TCT CAG CCA TCT G
	Reverse	GTC GCC AGC TTC AAC TAT TAA CT
Ccr7	Forward	TGT ACG AGT CGG TGT GCT TC
	Reverse	GGT AGG TAT CCG TCA TGG TCT TG
itgax	Forward	CTG GAT AGC CTT TCT TCT GCT G
	Reverse	GCA CAC TGT GTC CGA ACT C
Ccl2	Forward	TTA AAA ACC TGG ATC GGA ACC AA
	Reverse	GCA TTA GCT TCA GAT TTA CGG GT
Il6	Forward	TAG TCC TTC CTA CCC CAA TTT CC
	Reverse	TTG GTC CTT AGC CAC TCC TTC
Ifng	Forward	ATG AAC GCT ACA CAC TGC ATC
	Reverse	CCA TCC TTT TGC CAG TTC CTC
Foxp3	Forward	CCC ATC CCC AGG AGT CTT G
	Reverse	ACC ATG ACT AGG GGC ACT GTA